EURASIP Journal on Applied Signal Processing 2005:5, 718–729

Optimal Power Distribution Control for Multicode MC-CDMA with Zero-Forcing Successive Interference Cancellation

Mizhou Tan
Agere Systems, 1110 American Parkway NE, Allentown, PA 18109, USA
Email: mtan@agere.com

Christian Ibars
Centre Tecnològic de Telecomunicacions de Catalunya, C/Gran Capità 2-4, 08034 Barcelona, Spain
Email: christian.ibars@cttc.es

Yeheskel Bar-Ness
Center for Communications and Signal Processing Research (CCSPR), Department of Electrical and Computer Engineering (ECE), New Jersey Institute of Technology (NJIT), University Heights, Newark, NJ 07102, USA
Email: barness@yegal.njit.edu

Received 10 August 2003; Revised 11 March 2004

Multicarrier CDMA (MC-CDMA) has become a promising candidate for future wireless multimedia communications for its robustness to frequency-selective fading and its flexibility in handling multiple data rates. Among different multirate access schemes, multicode MC-CDMA is attractive for its high performance, good flexibility in rate matching, and low complexity. However, its performance is limited by self-interference (SI) and multiuser interference (MUI). In this paper, a zero-forcing successive interference cancellation (ZF-SIC) receiver is used to mitigate this problem for multicode MC-CDMA. Furthermore, optimal power distribution control (PDC), which minimizes each user's bit error rate (BER), is considered. Our results show that, in correlated Rayleigh fading channels, the ZF-SIC receiver integrated with the optimal PDC dramatically improves the performance of the multicode MC-CDMA system in comparison with other receivers proposed in the literature. Moreover, the optimal PDC significantly outperforms the PDC based on equal BER criterion, particularly under a short-term transmit power constraint.

Keywords and phrases: multicode, multicarrier CDMA, zero-forcing, successive interference cancellation, power distribution control.

1. INTRODUCTION

Multicarrier CDMA (MC-CDMA) combines multicarrier modulation (MCM) and DS-CDMA, and is characterized by its robustness to channel frequency selectivity and its simple receiver structure [1, 2, 3, 4]. Multirate MC-CDMA schemes were proposed to support multimedia applications in future wireless communications [5]. Multicode MC-CDMA is one of the multirate access schemes in which different symbols of each user are transmitted in parallel by employing different spreading codes. Compared with other multirate access schemes, multicode MC-CDMA presents better performance, higher rate matching capability, and lower complexity [6]. However, the capacity of MC-CDMA is mainly limited by self-interference (SI)[1] and multiuser interference (MUI). To mitigate this problem, many interference cancellation schemes have been proposed, among which successive interference cancellation (SIC) is highly desirable due to its ability to increase capacity while maintaining low complexity, its compatibility to existing systems, and its easy accommodation of strong error-correcting codes [7]. In this paper, a zero-forcing SIC (ZF-SIC) receiver is applied to multicode MC-CDMA, by which parallel symbols transmitted on different spreading codes are detected successively and, for each symbol (of the same or different users), a ZF receiver (decorrelator) is employed to eliminate interference. Such a detector is obtained with the Cholesky factorization (CF) of the cross-correlation matrix [8]. But unlike other detection techniques, SIC is sensitive to the receive power distribution. By providing perfect channel state information (CSI) at the receiver and error-free feedback from the receiver to the

[1] SI denotes the interference among different symbols of the same user.

transmitter,[2] it is possible to integrate SIC with power distribution control (PDC), which can improve system capacity significantly.

Since the integration of SIC and PDC was proposed for increasing system capacity, extensive research has been done in this area. Nevertheless, most of the work focused on a single-rate, single-carrier CDMA system with a matched filter (MF) SIC (MF-SIC) receiver. The equal bit error rate (BER) criterion, which is suitable for a system where all users aim to achieve comparable BER performances, was adopted in many references to derive the power distribution [7, 9, 10]. In [7], it is shown that, when ignoring decision errors, a geometric distribution of the receive power provides equal BER. In [9], equal BER performance is analyzed for linear SIC[3] in AWGN channels. In [10], with nonlinear SIC, the power distribution for equal BER is obtained using gradient search considering all error patterns. As it has been concluded in the literature, the equal BER PDC benefits SIC significantly by increasing the reliability of earlier detected users. However, in CDMA systems, with the increase of system load, the performance of the MF degrades quickly, which limits the effectiveness of the SIC. Hence, it is more meaningful to integrate PDC with SIC for more powerful detection techniques, such as ZF and minimum mean square error (MMSE).

In this paper, we investigate a PDC algorithm suitable for the nonlinear ZF-SIC receiver in a multicode MC-CDMA system. For such a system, PDC becomes more important than for a single-rate system, since without PDC it is customary to let the transmit power of each user be evenly distributed among all its spreading codes, which reduces the efficiency of SIC. Furthermore, as it is shown, the PDC for a multicode system requires a different approach from previously studied single-rate systems. In the multicode case the equal BER criterion only leads to a suboptimal solution for PDC; it forces equal BER for the symbols transmitted in parallel on different spreading codes of a given user, but it does not minimize its BER, which is the average over all parallel-transmitted symbols. Therefore, we propose an optimal PDC solution, that minimizes each user's BER while ensuring the same BER for different users. Both short-term and long-term transmit power constraints are considered. With a short-term power constraint, the transmit power is kept the same for every channel realization, while with a long-term constraint, the transmit power is adapted with channel variations [11]. Simulation results in correlated Rayleigh fading channels show a remarkable performance improvement for the multicode MC-CDMA system in comparison to other receivers proposed in the literature. Furthermore, the ZF-SIC with the optimal PDC significantly outperforms that with the equal BER PDC, particularly under the short-term power constraint.

Note that the proposed PDC scheme is of practical interest since it can also be easily adopted by a CDMA system with closed loop power control (CLPC), which adjusts transmit power among different users with a limited amount of feedback from the receiver, as a form of a vector of power-up and power-down bits.[4]

The remainder of this paper is organized as follows. The nonlinear ZF-SIC receiver for uplink multicode MC-CDMA is described in the next section. The equal BER PDC is discussed in Section 3 and is followed by the optimal PDC in Section 4, with the performances of both PDC strategies analyzed under short-term and long-term transmit power constraints. Simulation results are presented and discussed in Section 5. Finally, a conclusion is drawn.

2. NONLINEAR ZF-SIC RECEIVER FOR QUASISYNCHRONOUS UPLINK MC-CDMA

Consider a quasisynchronous uplink MC-CDMA in which all users are coordinated to transmit synchronously, with small, tolerated transmit time offsets. Signals received from different users have time offsets due to different propagation delays and channel delay spread. Symbol guard intervals larger than the maximum receive time offset are used to avoid intersymbol interference (ISI). The receiver is assumed synchronized to the user with the smallest delay. Thus, after discarding the guard intervals at the receiver, the quasisynchronous system can be analyzed as a synchronous system. To focus our attention on the ZF-SIC receiver, we assume no frequency offset and no nonlinear distortion.

With K active users in the system, the kth ($k = 1, 2, \ldots, K$) user is assigned l_k linearly independent spreading codes. With a total of N subcarriers, the number of utilized spreading codes is $L = \sum_{k=1}^{K} l_k \leq N$. The block diagram of the transmitter for the kth user is shown in Figure 1. As depicted in this figure, the data is first $1 : l_k$ serial-to-parallel (S/P) converted, then, each one of the parallel symbols is replicated into N copies and multiplied by a preassigned spreading code of length N (frequency domain spreading). After combining each chip of l_k symbols, a discrete-time multicarrier modulation is performed by an N-point IDFT. Then, after parallel-to-serial (P/S) conversion to form an OFDM symbol (time domain), a cyclic prefix of proper length Δ is inserted between successive symbols to avoid intersymbol interference (ISI). Finally, following radio frequency (RF) upconversion, the signal $s_k(t)$ is transmitted through the fading channel.

The complex equivalent lowpass transmit signal $s'_k(t)$ can be expressed as

$$s'_k(t) = \sum_{i=-\infty}^{+\infty} \sum_{l=1}^{l_k} \sum_{n=-N_g+1}^{N} a_{k,l} b_{k,l}(i) \times \sum_{m=1}^{N} c_{k,l,m} \cdot e^{j2\pi(mn/N)} p\left(\frac{t - iT'_s - nT'_s}{N + N_g}\right). \quad (1)$$

[2] We also assume that the channel is kept unchanged during the feedback.

[3] With linear SIC, soft decisions are employed for interference cancellation, while with nonlinear SIC, hard decisions are employed.

[4] Here, our approach makes no attempt at achieving capacity or spectrum optimization, as in [12, 13, 14], which requires a design of spreading codes or an allocation of power among different subcarriers optimally.

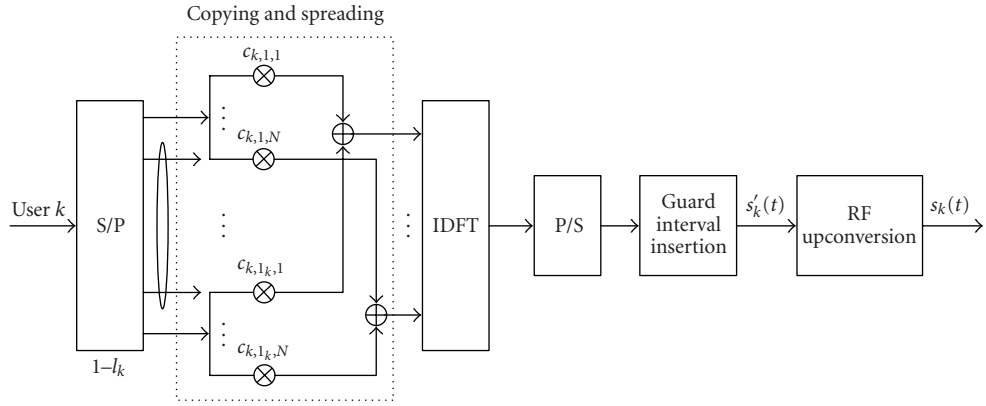

Figure 1: Block diagram of the transmitter of the kth user in uplink multicode MC-CDMA.

In the above equation, i denotes the ith OFDM symbol interval $[(i-1)T'_s, iT'_s)$, where $T'_s = T_s + \Delta$ and T_s is the effective OFDM symbol duration without insertion of a cyclic prefix. Subscript n denotes the nth sample (in the time domain) during each T'_s and m denotes the mth subcarrier. $N_g = N \cdot \Delta/T_s$ denotes the number of samples during each Δ. Also, $a_{k,l}, b_{k,l}(i) \in [1, -1]$ and $c_{k,l,m}$ denote the transmit signal amplitude, the ith BPSK-modulated symbol, and the mth chip of the lth spreading code $\mathbf{c}_{k,l}$ for the kth user, respectively. Finally, $p(t)$ is the rectangular pulse shape function.

A Rayleigh fading channel, corresponding to the worst case of no line-of-sight (LOS) component, is considered. By using a cyclic prefix of proper length, frequency-flat fading is obtained over each subcarrier [15]. With the assumption of time-invariant channel during each T'_s, for the kth user, the channel can be represented by an $(N \times 1)$ vector $\mathbf{h}_k$, given by

$$\mathbf{h}_k = \sqrt{g_k} \cdot \left[h_{k,1}, h_{k,2}, \ldots, h_{k,N}\right]^T, \tag{2}$$

where g_k denotes the path loss between the kth user and the base station, and $h_{k,n}$ represents the fading over the nth subcarrier, which is a complex Gaussian random variable with unit variance. In the uplink, different users' channels are assumed independent, identically distributed (i.i.d.). Furthermore, due to the proximity and partial overlap of the signal spectrum, correlated fading on different subcarriers is considered. The correlation between two subcarriers depends on the frequency spacing between them and the RMS channel delay spread τ_d [16, 17].

At the receiver, after RF downconversion and discarding the cyclic prefixes, the received signal $r'(t)$ can be expressed as

$$\begin{aligned} r'(t) = &\sum_{i=-\infty}^{+\infty} \sum_{k=1}^{K} \sum_{l=1}^{l_k} \sum_{n=1}^{N} a_{k,l} b_{k,l}(i) \\ &\times \sum_{m=1}^{N} \sqrt{g_k} h_{k,m} c_{k,l,m} \cdot e^{j2\pi(mn/N)} p\left(\frac{t - iT_s - nT_s}{N}\right) \\ &+ n(t), \end{aligned} \tag{3}$$

where the additive white complex Gaussian noise process $n(t)$ has zero mean and variance σ^2. After demodulation (DFT), the output during the ith effective OFDM symbol interval $[(i-1)T_s, iT_s)$ can be expressed in a compact matrix form as

$$\mathbf{x}(i) = \widetilde{\mathbf{C}}\mathbf{A}\mathbf{b}(i) + \boldsymbol{\eta}(i). \tag{4}$$

In (4), $\widetilde{\mathbf{C}}$ is the $(N \times L)$ spreading code matrix corrupted by the Rayleigh fading channels, expressed as $\widetilde{\mathbf{C}} = [\widetilde{\mathbf{C}}_1, \widetilde{\mathbf{C}}_2, \ldots, \widetilde{\mathbf{C}}_K]$, where the $(N \times l_k)$ matrix $\widetilde{\mathbf{C}}_k$ $(k = 1, 2, \ldots, K)$ is given by

$$\widetilde{\mathbf{C}}_k = [\widetilde{\mathbf{c}}_{k,1}, \widetilde{\mathbf{c}}_{k,2}, \ldots, \widetilde{\mathbf{c}}_{k,l_k}], \tag{5}$$

which contains l_k different code vectors of the kth user. Each item in (5) can be expressed as

$$\begin{aligned} \widetilde{\mathbf{c}}_{k,l} &= \mathbf{h}_k \odot \mathbf{c}_{k,l} \\ &= \sqrt{g_k}[h_{k,1}c_{k,l,1}, h_{k,2}c_{k,l,2}, \ldots, h_{k,N}c_{k,l,N}]^T. \end{aligned} \tag{6}$$

Additionally, $\mathbf{A}$ is an $(L \times L)$ diagonal matrix containing the transmit amplitudes of all symbols, given by

$$\mathbf{A} = \operatorname{diag}\left(\left[\mathbf{a}_1^T, \mathbf{a}_2^T, \ldots, \mathbf{a}_K^T\right]^T\right), \tag{7}$$

where $\operatorname{diag}(\cdot)$ denotes the diagonal matrix operator and $\mathbf{a}_k = [a_{k,1}, a_{k,2}, \ldots, a_{k,l_k}]^T$ $(k = 1, 2, \ldots, K)$. $\mathbf{b}(i)$ is an $(L \times 1)$ vector containing the parallel-transmitted symbols of all users with normalized power, given by

$$\mathbf{b}(i) = \left[\mathbf{b}_1^T(i), \mathbf{b}_2^T(i), \ldots, \mathbf{b}_K^T(i)\right]^T, \tag{8}$$

where $\mathbf{b}_k(i) = [b_{k,1}(i), b_{k,2}(i), \ldots, b_{k,l_k}(i)]^T$ $(k = 1, 2, \ldots, K)$. The $(N \times 1)$ white Gaussian noise vector $\boldsymbol{\eta}(i)$ has zero mean and covariance matrix $\sigma^2\mathbf{I}$, where $\mathbf{I}$ is an $(N \times N)$ identity matrix.

After the matched filter, we have

$$\begin{aligned} \mathbf{y}(i) &= \widetilde{\mathbf{C}}^H \cdot \mathbf{x}(i) \\ &= \mathbf{R}\mathbf{A}\mathbf{b}(i) + \widetilde{\boldsymbol{\eta}}(i), \end{aligned} \tag{9}$$

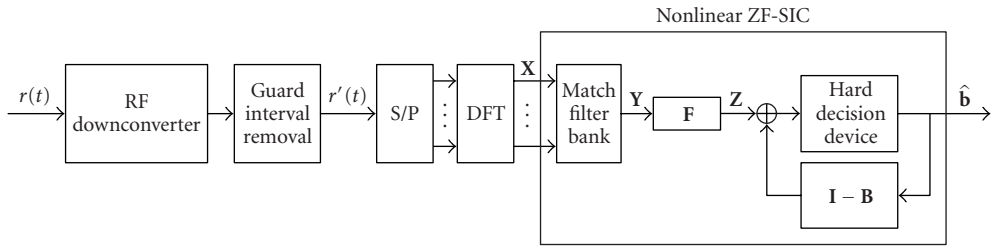

Figure 2: Block diagram of a nonlinear ZF-SIC receiver for multicode MC-CDMA.

for $l = 0$ to $L-1$

$$[\hat{\mathbf{b}}(i)]_{L-l} = \text{hard decision}\left([\mathbf{z}(i)]_{L-l} - \sum_{m=1}^{l}[\mathbf{A}]_{L-l+m,L-l+m}\cdot[\mathbf{\Gamma}]_{L-l,L-l+m}[\hat{\mathbf{b}}(i)]_{L-l+m}\right)$$

end

Algorithm 1

where we assume perfect CSI at the receiver. In the above equation, the cross-correlation matrix $\mathbf{R} = \tilde{\mathbf{C}}^H\tilde{\mathbf{C}}$ is positive definite in most cases. Hence, it can be uniquely decomposed as $\mathbf{R} = \mathbf{\Gamma}^H\mathbf{D}^2\mathbf{\Gamma}$, where $\mathbf{\Gamma}$ is upper triangular and monic (having all ones along the diagonal), and $\mathbf{D} = \text{diag}([\mathbf{d}_1^T, \mathbf{d}_2^T, \ldots, \mathbf{d}_K^T]^T)$ is a real $(L \times L)$ diagonal matrix, where $\mathbf{d}_k = [d_{k,1}, d_{k,2}, \ldots, d_{k,l_k}]^T$ $(k = 1, 2, \ldots, K)$. By multiplying both sides of (9) by $\mathbf{D}^{-2}\mathbf{\Gamma}^{-H}$, we obtain

$$\begin{aligned}\mathbf{z}(i) &= \mathbf{D}^{-2}\mathbf{\Gamma}^{-H}\cdot\mathbf{y}(i)\\ &= \mathbf{\Gamma}\mathbf{A}\mathbf{b}(i) + \hat{\boldsymbol{\eta}}(i),\end{aligned} \tag{10}$$

where $\hat{\boldsymbol{\eta}}(i)$ is an $(L \times 1)$ Gaussian vector with uncorrelated components, whose covariance matrix equals $\sigma_n^2\mathbf{D}^{-2}$ [8].

From (10), since $\mathbf{\Gamma}$ is upper triangular and $\hat{\boldsymbol{\eta}}(i)$ has uncorrelated components, the receive symbols $\hat{\mathbf{b}}(i) = [\hat{\mathbf{b}}_1^T(i), \hat{\mathbf{b}}_2^T(i), \ldots, \hat{\mathbf{b}}_K^T(i)]^T$can be recovered by back-substitution combined with symbol-by-symbol detection with Algorithm 1, where $[\mathbf{x}]_j$ and $[\mathbf{X}]_{i,j}$ denote the jth element of a vector $\mathbf{x}$ and the (i, j)th element of a matrix $\mathbf{X}$, respectively. The block diagram of the nonlinear ZF-SIC receiver is shown in Figure 2, where $\mathbf{F} \triangleq \mathbf{D}^{-2}\mathbf{\Gamma}^{-H}$ denotes the feedforward matrix, while $\mathbf{I} - \mathbf{B} \triangleq \mathbf{I} - \mathbf{\Gamma}$ denotes the feedback matrix.

From (10) and Algorithm 1, we see that the SNR γ_L of the first detected symbol $[\hat{\mathbf{b}}(i)]_L$ is the same as that of the ZF detector, given by [8]

$$\gamma_L = \frac{[\mathbf{A}^2]_{L,L}}{\sigma^2(\mathbf{R}^{-1})_{L,L}} = \frac{[\mathbf{A}^2]_{L,L}}{\sigma^2[\mathbf{D}^{-2}]_{L,L}}, \tag{11}$$

whereas other symbols are detected by subtracting a linear combination of previous hard decisions from $\mathbf{z}(i)$. In fact, the later detected symbols may contain interference from the earlier detected ones due to decision errors. Otherwise, if all cancellations are perfect, the performance of the last detected symbol achieves the single-user bound (SUB).

By ignoring decision errors, the sufficient statistic for the $(L-l)$th $(l = 0, 1, \ldots, L-1)$ symbol $[\mathbf{b}(i)]_{L-l}$ can simply be expressed as

$$[\mathbf{z}(i)]_{L-l} = [\mathbf{A}]_{L-l,L-l}[\mathbf{b}(i)]_{L-l} + [\hat{\boldsymbol{\eta}}(i)]_{L-l}, \tag{12}$$

and similar to (11), the SNR can be expressed as

$$\gamma_{L-l} = \frac{[\mathbf{A}^2]_{L-l,L-l}}{\sigma^2[\mathbf{D}^{-2}]_{L-l,L-l}}. \tag{13}$$

3. EQUAL BER PDC

With the equal BER criterion, each parallel-transmitted symbol achieves the same BER after the SIC. Clearly, the following equation should be satisfied:

$$\gamma_L = \gamma_{L-1} = \cdots = \gamma_1 \tag{14}$$

or

$$\frac{[\mathbf{A}^2]_{L,L}}{[\mathbf{D}^{-2}]_{L,L}} = \frac{[\mathbf{A}^2]_{L-1,L-1}}{[\mathbf{D}^{-2}]_{L-1,L-1}} = \cdots = \frac{[\mathbf{A}^2]_{1,1}}{[\mathbf{D}^{-2}]_{1,1}}. \tag{15}$$

3.1. Short-term transmit power constraint

Under each channel realization, the short-term transmit power constraint $\overline{\mathcal{P}}$ is defined as

$$\overline{\mathcal{P}} = \frac{1}{L}\text{tr}(\mathbf{A}^2), \tag{16}$$

where $\text{tr}(\mathbf{X})$ denotes the trace of a matrix $\mathbf{X}$. For a given channel realization, from (13) and (14), $\mathbf{A}$ must satisfy

$$[\mathbf{A}^2]_{L-l,L-l} = \gamma_{|h}\cdot\sigma^2[\mathbf{D}^{-2}]_{L-l,L-l} \quad (l = 0, 1, \ldots, L-1), \tag{17}$$

where $\gamma_{|h}$ denotes the achievable SNR, which depends on the channel realization. Applying (16), we have

$$\begin{aligned}\overline{\mathcal{P}} &= \frac{1}{L}\gamma_{|h}\sigma^2\cdot\sum_{l=0}^{L-1}[\mathbf{D}^{-2}]_{L-l,L-l}\\ &= \frac{1}{L}\gamma_{|h}\sigma^2\,\text{tr}\,(\mathbf{D}^{-2}).\end{aligned} \tag{18}$$

Therefore, $\gamma_{|h}$ can be expressed as

$$\gamma_{|h} = \frac{L\overline{\mathcal{P}}}{\sigma^2 \operatorname{tr}(\mathbf{D}^{-2})}, \tag{19}$$

and the power distribution is given by

$$[\mathbf{A}^2]_{L-l,L-l} = \frac{L[\mathbf{D}^{-2}]_{L-l,L-l}}{\operatorname{tr}(\mathbf{D}^{-2})}\overline{\mathcal{P}} \quad (l = 0, 1, \ldots, L-1). \tag{20}$$

Note that $\mathbf{A}$ and $\mathbf{D}$ also depend on the channel realization. We omit that in the notation for simplicity. Since decision errors are ignored, $\gamma_{|h}$ is higher than what can actually be achieved in the real system. Therefore, with the equal BER PDC, under the short-term power constraint, the average BER performance obtained with $\gamma_{|h}$ in (19) leads to a lower bound (LB) of the BER of the ZF-SIC receiver. For BPSK modulation, it can be expressed as

$$\begin{aligned} \mathrm{BER}_{\mathrm{LB-ST}} &= E_H[Q(\sqrt{\gamma_{|h}})] \\ &= E_H\left[Q\left(\sqrt{\frac{L\overline{\mathcal{P}}}{\sigma^2 \operatorname{tr}(\mathbf{D}^{-2})}}\right)\right], \end{aligned} \tag{21}$$

where $Q(\cdot)$ denotes the tail of the error function, and $E_H[\cdot]$ denotes the ensemble average over all channel realizations.

3.2. Long-term transmit power constraint

The long-term power constraint $\overline{\mathcal{P}}$ is determined by the average of powers over all channel realizations, which is

$$\overline{\mathcal{P}} = \frac{1}{L}E_H[\operatorname{tr}(\mathbf{A}^2)]. \tag{22}$$

Therefore, for a certain channel realization, we can define $\overline{\mathcal{P}}_{|h}$ as the required power for achieving a SNR γ (which is kept the same for all channel realizations), and from (18), we have

$$\overline{\mathcal{P}}_{|h} = \frac{1}{L}\gamma\sigma^2 \operatorname{tr}(\mathbf{D}^{-2}). \tag{23}$$

Substituting it into the power constraint expressed by (22), we obtain

$$\begin{aligned} \overline{\mathcal{P}} &= E_H[\overline{\mathcal{P}}_{|h}] \\ &= \frac{1}{L}\gamma\sigma^2 \cdot E_H[\operatorname{tr}(\mathbf{D}^{-2})]. \end{aligned} \tag{24}$$

The SNR γ for a long-term power constraint $\overline{\mathcal{P}}$ can be expressed as

$$\gamma = \frac{L\overline{\mathcal{P}}}{\sigma^2 E_H[\operatorname{tr}(\mathbf{D}^{-2})]}, \tag{25}$$

and the power distribution under each channel realization is given by

$$[\mathbf{A}^2]_{L-l,L-l} = \frac{L[\mathbf{D}^{-2}]_{L-l,L-l}}{E_H[\operatorname{tr}(\mathbf{D}^{-2})]}\overline{\mathcal{P}} \quad (l = 0, 1, \ldots, L-1). \tag{26}$$

Similarly, under the long-term power constraint, the LB for the equal BER PDC can be expressed as

$$\mathrm{BER}_{\mathrm{LB-LT}} = Q(\sqrt{\gamma}) = Q\left(\sqrt{\frac{L\overline{\mathcal{P}}}{\sigma^2 E_H[\operatorname{tr}(\mathbf{D}^{-2})]}}\right). \tag{27}$$

4. OPTIMAL PDC

With the equal BER PDC, the earlier detected symbols will be allocated more power since they are exposed to higher interference than the later detected ones. Hence, compared with the power distribution that ensures equal receive power, such an approach cancels interference more effectively by improving the reliability of symbols detected earlier. However, in a multicode system, the BER performance of each user is the average over all its parallel symbols transmitted on different spreading codes. That is, for the kth user, its BER performance is the average over all the l_k parallel transmit symbols, which can be expressed as

$$\overline{p}_{e,k}(\mathbf{a}_k^2) = \frac{1}{l_k}\sum_{l=1}^{l_k} p_{e,k,l}(a_{k,l}^2). \tag{28}$$

Therefore, from the viewpoint of minimizing BER, the equal BER PDC is only suboptimal. In this section, the optimal power distribution is derived based on the criterion of minimizing each user's BER.

4.1. Short-term transmit power constraint

With the short-term transmit power constraint $\overline{\mathcal{P}}$, under each channel realization, our optimization problem can be stated as follows. For the kth user, find the optimal power distribution $\mathbf{a}_k^{2*}$ which satisfies $\mathbf{a}_k^{2*} = \arg\min_{\mathbf{a}_k^2}(\overline{p}_{e,k}(\mathbf{a}_k^2))$ subject to

$$\begin{aligned} a_{k,l}^{2*} &\geq 0 \quad (l = 1, 2, \ldots, l_K), \\ \frac{1}{l_k}\sum_{l=1}^{l_k} a_{k,l}^{2*} &= \overline{\mathcal{P}}_k, \end{aligned} \tag{29}$$

where $\overline{\mathcal{P}}_k$ is the transmit power allocated to the kth user, which satisfies

$$\frac{1}{L}\sum_{k=1}^{K} l_k\overline{\mathcal{P}}_k = \overline{\mathcal{P}}. \tag{30}$$

Without loss of generality and for ease of comparison with the equal BER PDC, we assume different users have the same BER requirement, that is, $\overline{p}_{e,k}(\mathbf{a}_k^{2*}) = \overline{p}_{e,l}(\mathbf{a}_l^{2*})$ $(k, l = 1, 2, \ldots, K$ and $k \neq l)$. This determines the transmit power $\overline{\mathcal{P}}_k$ allocated to the kth $(k = 1, 2, \ldots, K)$ user, which will be explained later.

By ignoring cancellation errors, (28) can be rewritten as

$$\overline{p}_{e,k}(\mathbf{a}_k^2) = \frac{1}{l_k}\sum_{l=1}^{l_k} Q\left(\sqrt{\frac{a_{k,l}^2}{\sigma^2 \cdot d_{k,l}^{-2}}}\right). \tag{31}$$

It is clear that the BER minimization is a convex optimization problem with differentiable objects and constraint functions, for which a unique and global optimal solution exists. For the kth user, the optimal power distribution is found to be

$$a_{k,l}^{2*} = \begin{cases} -2d_{k,l}^{-2}\sigma^2 \ln\left(4\vartheta_k^* d_{k,l}^{-2}\sigma^2\right), & 0 < \vartheta_k^* < \dfrac{1}{4\sigma^2 d_{k,l}^{-2}}, \\ 0, & \vartheta_k^* \geq \dfrac{1}{4\sigma^2 d_{k,l}^{-2}}, \end{cases} \tag{32}$$

or equivalently,

$$a_{k,l}^{2*} = \max\left[0, -2d_{k,l}^{-2}\sigma^2 \ln\left(4\vartheta_k^* d_{k,l}^{-2}\sigma^2\right)\right], \tag{33}$$

where ϑ_k^* is the Lagrange multiplier, which can be found from the power constraint, expressed as

$$\frac{1}{l_k}\sum_{l=1}^{l_k} \max\left[0, -2d_{k,l}^{-2}\sigma^2 \ln\left(4\vartheta_k^* d_{k,l}^{-2}\sigma^2\right)\right] = \overline{\mathcal{P}}_k. \tag{34}$$

The Karush-Kuhn-Tucker (KKT) optimality conditions [18] are used to solve this problem, as shown in Appendix A. Also, for $\vartheta_k^* \in (0, 1/4\sigma^2 d_{k,l}^{-2}]$, $a_{k,l}^{2*} \in [0, +\infty)$ and it is monotonically decreasing with ϑ_k^*. Hence, for $\vartheta_k^* \in (0, \max_{l=1,2,\ldots,l_k}(1/4\sigma^2 d_{k,l}^{-2})]$, $\overline{\mathcal{P}}_k \in [0, +\infty)$ and also, it is monotonically decreasing with ϑ_k^*. Based on these conclusions and with (31), it is not difficult to find that $\overline{p}_{e,k}(\mathbf{a}_k^2)$ is monotonically decreasing with $\overline{\mathcal{P}}_k$.

For simplicity, considering only two users, under each channel realization, the algorithm can be summarized as follows. (1) Let $\overline{\mathcal{P}}_1 = \overline{\mathcal{P}}$ and let $\overline{\mathcal{P}}_2 = 0$. (2) Apply (34), ϑ_1^* and ϑ_2^* can be found. Then with (32), the power allocation $\mathbf{a}_1^{2*}$ and $\mathbf{a}_2^{2*}$ can be obtained. (3) Substitute $\mathbf{a}_1^{2*}$ and $\mathbf{a}_2^{2*}$ into (28), $\overline{p}_{e,1}(\mathbf{a}_1^{2*})$ and $\overline{p}_{e,2}(\mathbf{a}_2^{2*})$ can be obtained. (4) Compare $\overline{p}_{e,1}(\mathbf{a}_1^{2*})$ and $\overline{p}_{e,2}(\mathbf{a}_2^{2*})$; if $\overline{p}_{e,1}(\mathbf{a}_1^{2*}) < \overline{p}_{e,2}(\mathbf{a}_2^{2*})$, let $\overline{\mathcal{P}}_1 = \overline{\mathcal{P}}_1 - \Delta\overline{\mathcal{P}}$ and $\overline{\mathcal{P}}_2 = \overline{\mathcal{P}}_2 + \Delta\overline{\mathcal{P}}$, and go back to (2) until finally, $\overline{p}_{e,1}(\mathbf{a}_1^{2*}) = \overline{p}_{e,2}(\mathbf{a}_2^{2*})$ with predefined accuracy. This algorithm can be extended to the scenario where the number of users is greater than two.[5] As in the previous section, since decision errors are ignored, then for the kth ($k = 1, 2, \ldots, K$) user, the LB of the proposed optimal PDC, under the short-term power constraint can be expressed as

$$\mathrm{BER}_{\mathrm{LB-ST}}^{(k)} = \frac{1}{l_k} E_H\left[\sum_{l=1}^{l_k} Q\left(\sqrt{\frac{a_{k,l}^{2*}}{\sigma^2 \cdot d_{k,l}^{-2}}}\right)\right]. \tag{35}$$

[5]With a large number of users, the complexity of the search algorithm might become high. However, in practice, the power constraint on all users can be relaxed to a separated power constraint on each user, under which the optimal PDC can easily be derived.

4.2. Long-term transmit power constraint

With the long-term power constraint $\overline{\mathcal{P}}$, the optimization problem can be stated as follows. For the kth user, find the optimal power distribution $\mathbf{a}_k^{2*}$ which satisfies $\mathbf{a}_k^{2*} = \arg\min_{\mathbf{a}_k^2}(E_H[\overline{p}_{e,k}(\mathbf{a}_k^2)])$ subject to

$$\begin{aligned} a_{k,l}^{2*} &\geq 0 \quad (l = 1, 2, \ldots, l_K), \\ E_H\left[\frac{1}{l_k}\sum_{l=1}^{l_k} a_{k,l}^{2*}\right] &= \overline{\mathcal{P}}_k, \end{aligned} \tag{36}$$

where $E_H[\overline{p}_{e,k}(\mathbf{a}_k^2)]$ denotes the BER of the kth user, averaged over all channel realizations, given by

$$E_H[\overline{p}_{e,k}(\mathbf{a}_k^2)] = E_H\left[\frac{1}{l_k}\sum_{l=1}^{l_k} p_{e,k,l}(a_{k,l}^2)\right]. \tag{37}$$

Similarly, $\overline{\mathcal{P}}_k$ satisfies (30).

After solving the KKT optimality conditions, shown in Appendix B, we obtain the optimal power distribution for the kth user, which is expressed exactly as (32) or (33), while ϑ_k^* is obtained from the following power constraint:

$$\frac{1}{l_k} E_H\left[\sum_{l=1}^{l_k} \max\left[0, -2d_{k,l}^{-2}\sigma^2 \ln\left(4\vartheta_k^* d_{k,l}^{-2}\sigma^2\right)\right]\right] = \overline{\mathcal{P}}_k, \tag{38}$$

instead of (34). A similar algorithm as stated in the previous subsection can be applied, but in this case, ϑ_k^* is found over all channel realizations. Also, under the long-term power constraint, for the kth user, the LB of the optimal PDC over all channel realizations is given by

$$\mathrm{BER}_{\mathrm{LB-LT}}^{(k)} = \frac{1}{l_k} E_H\left[\sum_{l=1}^{l_k} Q\left(\sqrt{\frac{a_{k,l}^{2*}}{\sigma^2 \cdot d_{k,l}^{-2}}}\right)\right]. \tag{39}$$

From the above analyses, it can be found that with the optimal PDC, when $d_{k,l}^{-2} \geq 1/4\sigma^2\vartheta_k^*$ (ϑ_k^* has to be determined), no power will be allocated to the lth symbol of the kth user, which implies that, unlike the equal BER PDC, which always consumes more power to compensate for higher noise power[6] for achieving the same SNR, the optimal PDC allocates no power to those symbols whose noise power is equal to or higher than a certain level ($1/4\sigma^2\vartheta_k^*$), while allocating more power for other "better" symbols, to ensure more reliable transmissions. Also, for those symbols whose noise power is less than a certain level ($1/4\sigma^2\vartheta_k^*$), then from (32), under a chosen ϑ_k^*, since $a_{k,l}^{2*}$ is monotonically increasing with $d_{k,l}^{-2}$, more power will be allocated to the symbols with higher noise power to ensure the reliability of earlier detected symbols. These two different PDC strategies, the equal BER PDC, and the optimal PDC result in different BER performances, which will be presented in the next section.

[6]From (13), $d_{k,l}^{-2}$ can be looked upon as the noise power with $\sigma^2 = 1$.

Table 1 Simulation parameters.

Parameters	Values in simulations
Bandwidth	100 MHz
τ_d	25 ns
N	16
g	$g = g_1 = g_2 = \cdots = g_K = 1$
Modulation	BPSK
Number of channels	1000
Symbols for each channel	160

5. SIMULATION RESULTS AND DISCUSSIONS

An indoor-correlated Rayleigh fading channel model is employed in the simulations. The total available bandwidth is 100 MHz, with $\tau_d = 25$ nanoseconds, and the number of subcarriers is 16. Without loss of generality, the path loss of different users is assumed equal, denoted by g and $g = g_1 = \cdots = g_K = 1$. We consider here only uncoded MC-CDMA with Walsh Hadamard spreading codes. For simplicity, we assume two users, each employing 8 codes in the fully loaded system, and a slow fading channel, constant over a frame of 160 BPSK-modulated symbols. All simulation results are obtained over 1000 channel realizations. For easy reference, the simulation parameters are included in Table 1. Besides showing the performance of the ZF-SIC receiver integrated with the optimal PDC and equal BER PDC discussed in this paper, the performance of the ZF receiver without SIC and the ZF-SIC receiver without PDC are also presented for comparison. In these cases, the transmit power is equally distributed among all parallel-transmitted symbols of each user. Furthermore, the performance of the nonlinear MF-SIC with the equal BER PDC, proposed in the literature, is also compared.

Under the short-term power constraint, the BER performance *averaged over two users*[7] versus E_b/N_0[8] in the fully loaded system is shown in Figure 3. From this figure, it is clear that the ZF receiver without employing SIC, (a), cannot compensate channel fading very well. By employing SIC, even with equal transmit power (no PDC), (b), the performance can be improved significantly. Further improvement is obtained with the equal BER PDC, (c); at a BER of 10^{-3}, another 3.5 dB performance improvement can be obtained.[9] Moreover, for both with equal BER PDC, the ZF-SIC, (c), suppresses interference more effectively than the MF-SIC, (d). Not surprisingly, the optimal PDC, (e), significantly outperforms the equal BER PDC, (c); at a BER of 10^{-3}, an extra 2 dB performance improvement can be obtained. For comparison, the LBs based on (21), (f), and (35), (g), and the SUB, under short-term power constraint, are plotted in this

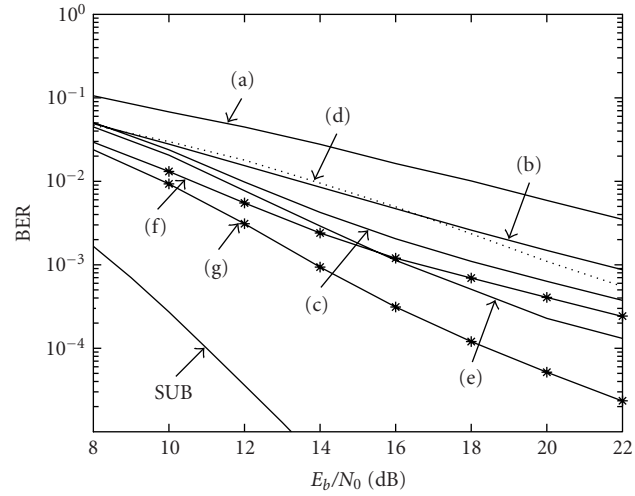

Figure 3: BER performance (averaged over two users) in the fully loaded system under a short-term power constraint ((a) ZF (no SIC), (b) ZF-SIC (no PDC), (c) ZF-SIC (equal BER), (d) MF-SIC (equal BER), (e) ZF-SIC (optimal), (f) LB (equal BER, (21)), (g) LB (optimal, (35))).

figure. It can also be easily found that the performance difference between the LBs and the actual simulation results is quite large, which might be due to the fact that decision errors which were ignored have a significant effect on the BER performance. Also, since the optimal PDC is only optimal under the assumption of error-free decisions, if such errors could be properly taken into consideration the performance might have further improved, particularly for the ZF-SIC with the optimal PDC.

The BER performances of *the two sequentially detected users* with SIC are compared in Figure 4. For the ZF-SIC receiver, with equal transmit power (no PDC), the performance difference between two users is very large; the second detected user achieves much better performance than the first one, since more interference has been cancelled. With the equal BER PDC, the performance of two users becomes close with increasing E_b/N_0, because the decision errors have nearly the same effects on both. With the optimal PDC, two users achieve very similar performance, which is superior to that with the equal BER PDC. It is also interesting to note that with both the equal BER PDC and optimal PDC, the first detected user can achieve slightly better performance than the second one, because the PDC ignoring decision errors results in lower power for the later detected user than it actually needs [9]. For the MF-SIC, even with the equal BER PDC, the performance difference between two users is quite large, which means decision errors might have a larger effect on it than on the ZF-SIC.

Under the long-term power constraint, the BER performance *averaged over two users* in the fully loaded system is shown in Figure 5. Compared to the results shown in Figure 3, in this case channel fading can be compensated more effectively at high E_b/N_0. With equal transmit power (no PDC), at a BER of 10^{-3}, the ZF-SIC receiver, (b), only obtains 1 dB performance improvement from the ZF receiver

[7] Since both users aim to achieve the same BER, the average performance over the two users can be employed for comparison.

[8] E_b/N_0 is the average SNR per bit, defined as $E_b/N_0 = 10\log_{10}\overline{\mathcal{P}}/2\sigma^2$ (dB).

[9] A BER of 10^{-3} is considered for the uncoded MC-CDMA system, which could be easily translated into a BER of 10^{-6}, when a moderate channel coding scheme is employed.

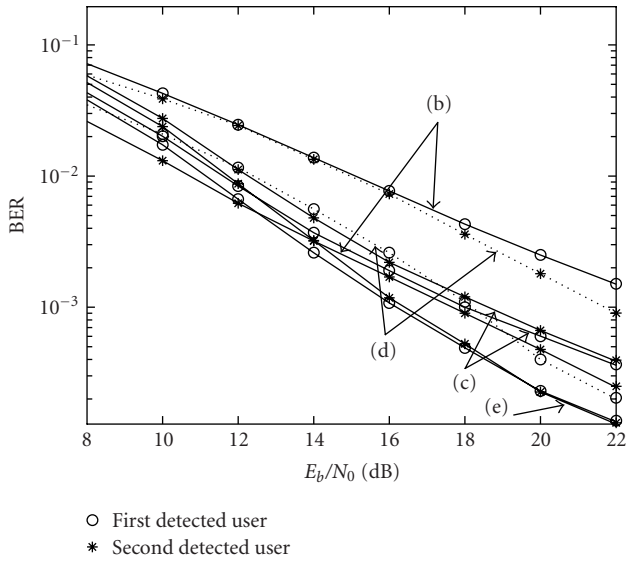

Figure 4: BER performance of two sequentially detected users in the fully loaded system under a short-term power constraint ((b) ZF-SIC (no PDC), (c) ZF-SIC (equal BER), (d) MF-SIC (equal BER), (e) ZF-SIC (optimal)).

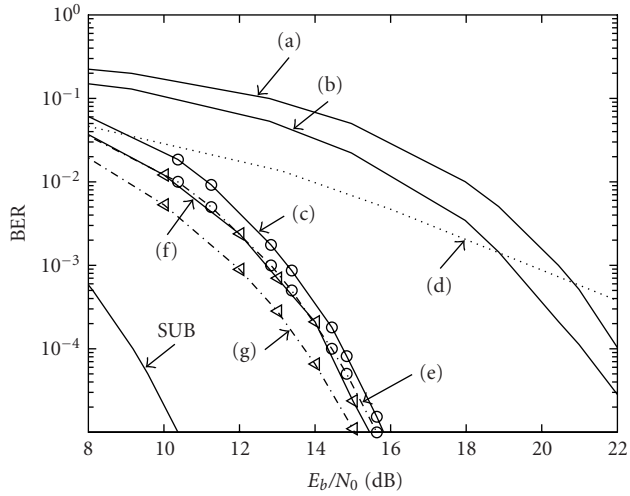

Figure 5: BER performance (averaged over two users) in the fully loaded system under a long-term power constraint ((a) ZF (no SIC), (b) ZF-SIC (no PDC), (c) ZF-SIC (equal BER), (d) MF-SIC (equal BER), (e) ZF-SIC (optimal), (f) LB (equal BER, (27)), (g) LB (optimal, (39))).

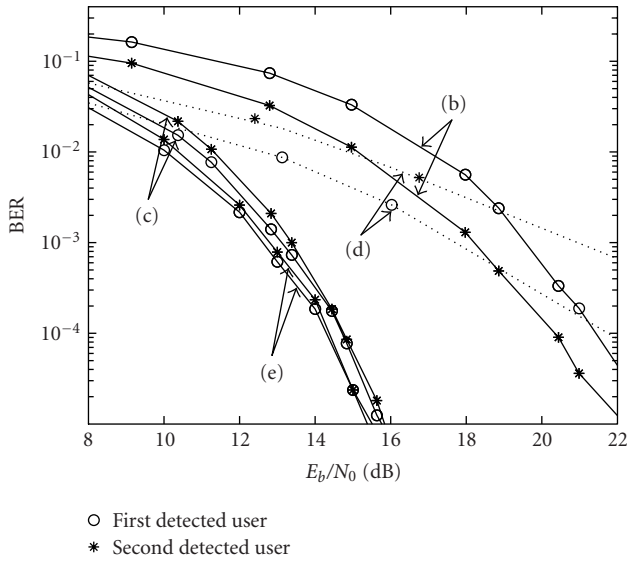

Figure 6: BER performance of two sequentially detected users in the fully loaded system under a long-term power constraint ((b) ZF-SIC (no PDC), (c) ZF-SIC (equal BER), (d) MF-SIC (equal BER), (e) ZF-SIC (optimal)).

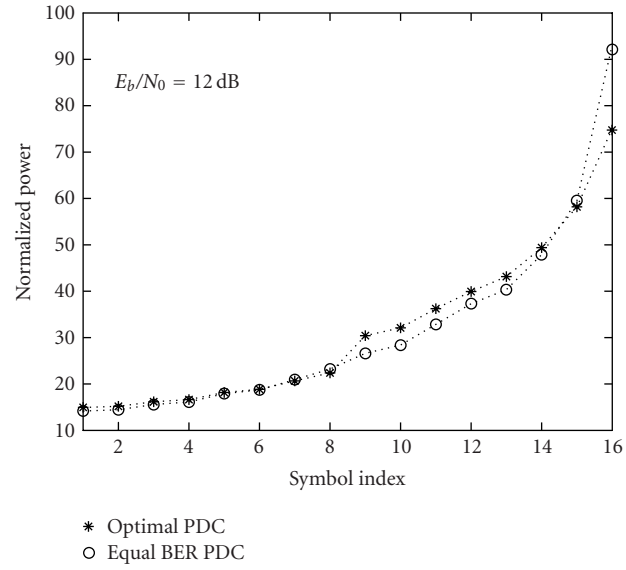

Figure 7: Normalized transmit power distribution (averaged over 1000 channel realizations) on 16 parallel-transmitted symbols under a short-term power constraint.

without SIC, (a). However, by integrating PDC with ZF-SIC, a dramatic performance improvement can be achieved. With the equal BER PDC, the ZF-SIC, (c), obtains about 6 dB performance improvement at a BER of 10^{-3}, much better than the MF-SIC with the equal BER PDC, (d). Furthermore, it can be seen that the optimal PDC, (e), outperforms the equal BER PDC, (c). The LBs based on (27), (f), and (39), (g), and the SUB, under the long-term power constraint, are also shown for comparison. We note that in this case the performance difference between the LBs and the actual simulation results is within 0.2–0.6 dB, which implies as argued earlier that the performance loss caused by ignoring decision errors is almost negligible. The BER performances of *the two sequentially detected users* with SIC is compared in Figure 6, from which conclusions similar to Figure 4 can be obtained.

In Figures 7 and 8, the normalized transmit power (divided by σ^2) distribution, among the 16 symbols transmitted in parallel on different spreading codes is shown for the short-term and long-term power constraints, with

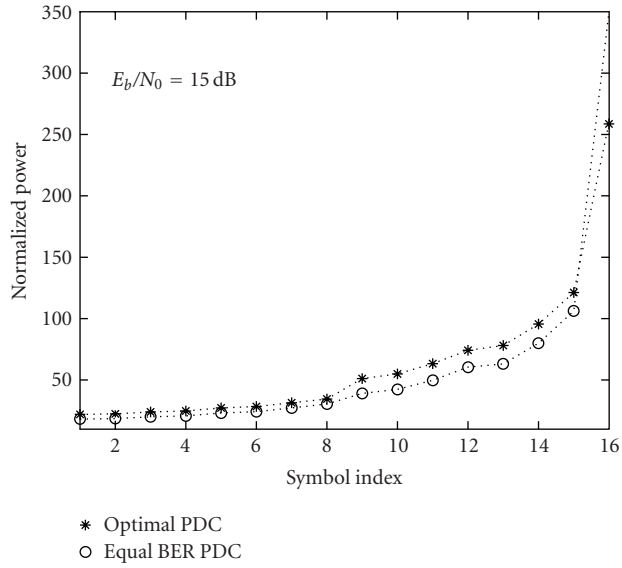

FIGURE 8: Normalized transmit power distribution (averaged over 1000 channel realizations) on 16 parallel-transmitted symbols under a long-term power constraint.

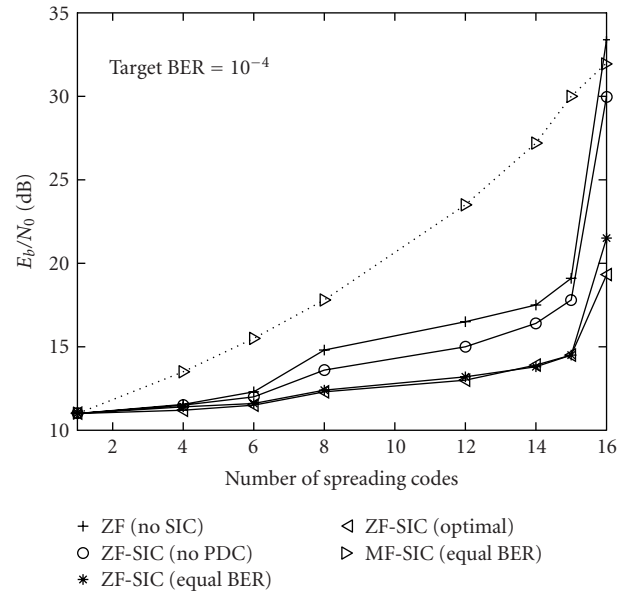

FIGURE 9: Required E_b/N_0 for achieving a target BER of 10^{-4} versus different system load under a short-term power constraint.

average E_b/N_0 12 dB and 15 dB, respectively. In these two figures, larger indexes denote earlier detected symbols. For all schemes, under the chosen E_b/N_0, it was found that earlier detected symbols are allocated more power than later detected ones. However, it is interesting to note that, compared with the equal BER PDC, the optimal PDC allocated less power to earlier detected symbols and more to later detected ones. This compensates for a certain performance loss caused by underestimating the required power of later detected symbols with the equal BER PDC, resulting in a better performance.

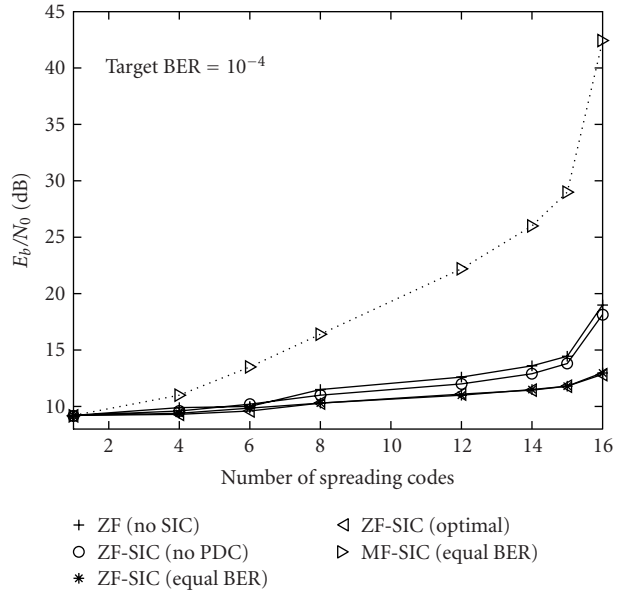

FIGURE 10: Required E_b/N_0 for achieving a target BER of 10^{-4} versus different system load under a long-term power constraint.

In the previous figures, the performance of the fully loaded system was studied. Alternatively, in Figures 9 and 10, the required E_b/N_0 versus the number of spreading codes is shown for the short-term and long-term power constraints, respectively, at a target BER of 10^{-4}. For simplicity in these two figures we assumed a single user with a variable number of spreading codes. When only one code is employed, the system can be looked upon as a single-user system, while when 16 codes are employed, it is equivalent to a fully loaded system. From these results we found that, when increasing the system load, the performance of the MF-SIC with the equal BER PDC degrades very quickly. Furthermore, the ZF-SIC receiver integrated with the optimal PDC needs the smallest power, particularly under the short-term power constraint and when the system is highly loaded.

6. CONCLUSIONS

A nonlinear ZF-SIC receiver was applied for multicode MC-CDMA and a solution of optimal PDC was presented. Under the assumption of perfect CSI at the receiver and error-free feedback from the receiver to the transmitter, the performance of the ZF-SIC with the optimal PDC was investigated and compared with the equal BER PDC, for both short-term and long-term transmit power constraints. Simulation results obtained in correlated Rayleigh fading channels show the effectiveness of the optimal PDC and its superior performance to the equal BER PDC. Moreover, optimal PDC combined with ZF-SIC significantly outperforms the MF-SIC with the equal BER PDC proposed in the literature. To further improve the performance with SIC, the optimal decision feedback receiver MMSE-SIC [19] integrated with PDC seems a promising solution to be investigated in future work.

APPENDICES

A. SOLUTIONS OF KKT OPTIMALITY CONDITIONS UNDER A SHORT-TERM TRANSMIT POWER CONSTRAINT

To solve the optimization problem under a short-term power constraint we introduce Lagrange multipliers $\boldsymbol{\lambda}_k = [\lambda_{k,1}, \lambda_{k,2}, \ldots, \lambda_{k,l_k}]^T$ for the inequality constraints, $a_{k,l}^2 \geq 0$ $(l = 1, 2, \ldots, l_K)$, and ϑ_k for the equality constraint $(1/l_k)\sum_{l=1}^{l_k} a_{k,l}^2 = \overline{\mathcal{P}}_k$. Hence, the Lagrangian is given by

$$\mathcal{L}(\mathbf{a}_k^2, \boldsymbol{\lambda}, \vartheta_k) = \overline{p}_{e,k}(\mathbf{a}_k^2) - \sum_{l=1}^{l_k} \lambda_{k,l} a_{k,l}^2 + \vartheta_k \left(\frac{1}{l_k} \sum_{l=1}^{l_k} a_{k,l}^2 \right). \quad \text{(A.1)}$$

With the approximation of $Q(x) \approx (1/2)\exp(-x^2/2)$, $\overline{p}_{e,k}(\mathbf{a}_k^2)$ can be expressed as

$$\begin{aligned} \overline{p}_{e,k}(\mathbf{a}_k^2) &= \frac{1}{l_k} \sum_{l=1}^{l_k} Q\left(\sqrt{\frac{a_{k,l}^2}{\sigma^2 \cdot d_{k,l}^{-2}}} \right) \\ &\approx \frac{1}{l_k} \sum_{l=1}^{l_k} \frac{1}{2} \exp\left(-\frac{a_{k,l}^2}{2\sigma^2 \cdot d_{k,l}^{-2}} \right). \end{aligned} \quad \text{(A.2)}$$

Therefore, the KKT optimality conditions can be expressed as [18]

$$\begin{gathered} \boldsymbol{\lambda}_k^* \geq \mathbf{0}, \quad \text{i.e., } \lambda_{k,l}^* \geq 0, \\ \frac{1}{l_k} \sum_{l=1}^{l_k} a_{k,l}^{2*} = \overline{\mathcal{P}}_k, \quad a_{k,l}^{2*} \geq 0, \\ \frac{1}{l_k} \cdot \frac{1}{2} \exp\left(-\frac{a_{k,l}^2}{2\sigma^2 \cdot d_{k,l}^{-2}} \right) \cdot \left(-\frac{1}{2\sigma^2 \cdot d_{k,l}^{-2}} \right) - \lambda_{k,l}^* + \frac{1}{l_k} \vartheta_k^* = 0, \\ \lambda_{k,l}^* \cdot a_{k,l}^{2*} = 0 \\ (l = 1, 2, \ldots, l_K). \end{gathered} \quad \text{(A.3)}$$

The third equation in (A.3) is obtained by differentiating the right side of (A.1) with respect to $a_{k,l}^{2*}$ and setting it to zero. We note that $\lambda_{k,l}^*$ acts as a slack variable in the third equation, so it can be eliminated, leaving

$$\begin{gathered} \boldsymbol{\lambda}_k^* \geq \mathbf{0}, \quad \text{i.e., } \lambda_{k,l}^* \geq 0, \\ \frac{1}{l_k} \sum_{l=1}^{l_k} a_{k,l}^{2*} = \overline{\mathcal{P}}_k, \quad a_{k,l}^{2*} \geq 0, \\ \vartheta_k^* \geq \frac{1}{2} \exp\left(-\frac{a_{k,l}^2}{2\sigma^2 \cdot d_{k,l}^{-2}} \right) \cdot \frac{1}{2\sigma^2 \cdot d_{k,l}^{-2}}, \\ a_{k,l}^{2*} \cdot \left(\vartheta_k - \frac{1}{2} \exp\left(-\frac{a_{k,l}^2}{2\sigma^2 \cdot d_{k,l}^{-2}} \right) \cdot \frac{1}{2\sigma^2 \cdot d_{k,l}^{-2}} \right) = 0 \\ (l = 1, 2, \ldots, l_K). \end{gathered} \quad \text{(A.4)}$$

If $0 < \vartheta_k^* < 1/4\sigma^2 d_{k,l}^{-2}$, then for $a_{k,l}^{2*} = 0$, the third equation cannot hold, and with $a_{k,l}^{2*} > 0$, the last condition implies that $a_{k,l}^{2*} = -2d_{k,l}^{-2}\sigma^2 \ln(4\vartheta_k^* d_{k,l}^{-2}\sigma^2)$. If $\vartheta_k^* \geq 1/4\sigma^2 d_{k,l}^{-2}$, then $a_{k,l}^{2*} > 0$ leads to a nonzero term in the parenthesis of the fourth equation which contradicts the equality, thus, $a_{k,l}^{2*} = 0$. Therefore, we have

$$a_{k,l}^{2*} = \begin{cases} -2d_{k,l}^{-2}\sigma^2 \ln\left(4\vartheta_k^* d_{k,l}^{-2}\sigma^2\right), & 0 < \vartheta_k^* < \dfrac{1}{4\sigma^2 d_{k,l}^{-2}}, \\ 0, & \vartheta_k^* \geq \dfrac{1}{4\sigma^2 d_{k,l}^{-2}}, \end{cases} \quad \text{(A.5)}$$

or equivalently,

$$a_{k,l}^{2*} = \max\left[0, -2d_{k,l}^{-2}\sigma^2 \ln\left(4\vartheta_k^* d_{k,l}^{-2}\sigma^2\right)\right]. \quad \text{(A.6)}$$

Substituting this expression for $a_{k,l}^{2*}$ into the average power constraint condition, we obtain

$$\frac{1}{l_k} \sum_{l=1}^{l_k} \max\left[0, -2d_{k,l}^{-2}\sigma^2 \ln\left(4\vartheta_k^* d_{k,l}^{-2}\sigma^2\right)\right] = \overline{\mathcal{P}}_k. \quad \text{(A.7)}$$

Note that when $0 < \vartheta_k^* < 1/4\sigma^2 d_{k,l}^{-2}$, each one of the l_k functions is monotonically decreasing with ϑ_k^*, and when $\vartheta_k^* \geq 1/4\sigma^2 d_{k,l}^{-2}$, it becomes zero, so the equation has a unique solution ϑ_k^* which is readily determined. Hence, the optimal power distribution can be obtained.

B. SOLUTIONS OF KKT OPTIMALITY CONDITIONS UNDER A LONG-TERM TRANSMIT POWER CONSTRAINT

To solve the optimization problem under a long-term average power constraint, the Lagrangian is given by

$$\begin{aligned} \mathcal{L}(\mathbf{a}_k^2, \boldsymbol{\lambda}_k, \vartheta_k) &= E_H[\overline{p}_{e,k}(\mathbf{a}_k^2)] \\ &\quad - \sum_{l=1}^{l_k} \lambda_{k,l} a_{k,l}^2 + \vartheta_k \left(E_H\left[\frac{1}{l_k} \sum_{l=1}^{l_k} a_{k,l}^2 \right] \right). \end{aligned} \quad \text{(B.1)}$$

Similarly, the KKT optimality conditions are expressed as

$$\begin{gathered} \boldsymbol{\lambda}_k^* \geq \mathbf{0}, \quad \text{i.e., } \lambda_{k,l}^* \geq 0, \\ \frac{1}{l_k} \int \rho_H(\mathbf{h}_k) \cdot \sum_{l=1}^{l_k} a_{k,l}^{2*} d\mathbf{h}_k = \overline{\mathcal{P}}_k, \quad a_{k,l}^{2*} \geq 0, \\ \frac{1}{l_k} \int \rho_H(\mathbf{h}_k) \cdot \frac{1}{2} \exp\left(-\frac{a_{k,l}^{2*}}{2\sigma^2 \cdot d_{k,l}^{-2}} \right) \\ \cdot \left(-\frac{1}{2\sigma^2 \cdot d_{k,l}^{-2}} \right) d\mathbf{h}_k - \lambda_{k,l}^* + \frac{1}{l_k} \int \rho_H(\mathbf{h}_k) \cdot \vartheta_k^* d\mathbf{h}_k = 0, \\ \lambda_{k,l}^* \cdot a_{k,l}^{2*} = 0 \\ (l = 1, 2, \ldots, l_K). \end{gathered} \quad \text{(B.2)}$$

After eliminating the slack variable $\lambda_{k,l}^*$ in the third equation, we have

$$\begin{aligned}
&\boldsymbol{\lambda}_k^* \geq \mathbf{0}, \quad \text{i.e., } \lambda_{k,l}^* \geq 0,\\
&\frac{1}{l_k}\int \rho_H(\mathbf{h}_k)\cdot\sum_{l=1}^{l_k} a_{k,l}^{2*}\,d\mathbf{h}_k = \overline{\mathcal{P}}_k, \quad a_{k,l}^{2*} \geq 0,\\
&\int \rho_H(\mathbf{h}_k)\cdot\vartheta_k d\mathbf{h}_k \geq \int \rho_H(\mathbf{h}_k)\cdot\frac{1}{2}\exp\left(-\frac{a_{k,l}^{2*}}{2\sigma^2\cdot d_{k,l}^{-2}}\right)\\
&\qquad\cdot\left(-\frac{1}{2\sigma^2\cdot d_{k,l}^{-2}}\right)d\mathbf{h}_k,\\
&a_{k,l}^{2*}\cdot\left\{\int \rho_H(\mathbf{h}_k)\cdot\left(\vartheta_k-\frac{1}{2}\exp\left(-\frac{a_{k,l}^{2*}}{2\sigma^2\cdot d_{k,l}^{-2}}\right)\right.\right.\\
&\qquad\left.\left.\cdot\frac{1}{2\sigma^2\cdot d_{k,l}^{-2}}\right)d\mathbf{h}_k\right\} = 0\\
&\qquad(l=1,2,\ldots,l_K).
\end{aligned} \tag{B.3}$$

With similar analysis as in Appendix A, we have

$$a_{k,l}^{2*} = \begin{cases} -2d_{k,l}^{-2}\sigma^2\ln\left(4\vartheta_k^* d_{k,l}^{-2}\sigma^2\right), & 0<\vartheta_k^*<\dfrac{1}{4\sigma^2 d_{k,l}^{-2}},\\ 0, & \vartheta_k^*\geq\dfrac{1}{4\sigma^2 d_{k,l}^{-2}}, \end{cases} \tag{B.4}$$

or equivalently,

$$a_{k,l}^{2*} = \max\left[0, -2d_{k,l}^{-2}\sigma^2\ln\left(4\vartheta_k^* d_{k,l}^{-2}\sigma^2\right)\right]. \tag{B.5}$$

Substituting this expression for $a_{k,l}^{2*}$ into the average power constraint, we obtain

$$\int \rho_H(\mathbf{h}_k)\cdot\sum_{l=1}^{l_k}\max\left[0,-2d_{k,l}^{-2}\sigma^2\ln\left(4\vartheta_k^* d_{k,l}^{-2}\sigma^2\right)\right]d\mathbf{h}_k = \overline{\mathcal{P}}_k, \tag{B.6}$$

from which ϑ_k^* can be solved.[10] Hence, the optimal power distribution can be obtained.

ACKNOWLEDGMENT

This work was partially supported by NSF Grant CCR-0085846.

[10] To solve the integral, a summation over the ensemble of channel realizations is used as an approximation.

REFERENCES

[1] N. Yee, J.-P. Linnartz, and G. Fettweis, "Multi-carrier CDMA in indoor wireless radio networks," in *Proc. 4th IEEE International Symposium on Personal, Indoor and Mobile Radio Communications (PIMRC '93)*, pp. 109–113, Yokohama, Japan, September 1993.

[2] S. Hara and R. Prasad, "Overview of multicarrier CDMA," *IEEE Commun. Mag.*, vol. 35, no. 12, pp. 126–133, 1997.

[3] E. A. Sourour and M. Nakagawa, "Performance of orthogonal multicarrier CDMA in a multipath fading channel," *IEEE Trans. Commun.*, vol. 44, no. 3, pp. 356–367, 1996.

[4] S. Hara and R. Prasad, "Design and performance of multicarrier CDMA system in frequency-selective Rayleigh fading channels," *IEEE Trans. Veh. Technol.*, vol. 48, no. 5, pp. 1584–1595, 1999.

[5] M. Tan and Y. Bar-Ness, "Multi-rate access schemes for wireless multimedia MC-CDMA communications," submitted to *IEEE Commun. Mag.,* July 2003.

[6] M. Tan, P. Zong, and Y. Bar-Ness, "Multi-rate access schemes for MC-CDMA," *International Journal of Wireless Personal Communications*, vol. 27, no. 2, pp. 149–182, 2003.

[7] A. J. Viterbi, "Very low rate convolution codes for maximum theoretical performance of spread-spectrum multiple-access channels," *IEEE J. Select. Areas Commun.*, vol. 8, no. 4, pp. 641–649, 1990.

[8] A. Duel-Hallen, "Decorrelating decision-feedback multiuser detector for synchronous code-division multiple-access channel," *IEEE Trans. Commun.*, vol. 41, no. 2, pp. 285–290, 1993.

[9] R. M. Buehrer, "Equal BER performance in linear successive interference cancellation for CDMA systems," *IEEE Trans. Commun.*, vol. 49, no. 7, pp. 1250–1258, 2001.

[10] G. Mazzini, "Equal BER with successive interference cancellation DS-CDMA systems on AWGN and Ricean channels," in *Proc. 6th IEEE International Symposium on Personal, Indoor and Mobile Radio Communications (PIMRC '95)*, vol. 2, pp. 727–731, Toronto, Ontario, Canada, September 1995.

[11] A. J. Goldsmith and P. P. Varaiya, "Capacity of fading channels with channel side information," *IEEE Trans. Inform. Theory*, vol. 43, no. 6, pp. 1986–1992, 1997.

[12] D. N. C. Tse and S. V. Hanly, "Multiaccess fading channels. I. Polymatroid structure, optimal resource allocation and throughput capacities," *IEEE Trans. Inform. Theory*, vol. 44, no. 7, pp. 2796–2815, 1998.

[13] S. V. Hanly and D. N. C. Tse, "Multiaccess fading channels. II. Delay-limited capacities," *IEEE Trans. Inform. Theory*, vol. 44, no. 7, pp. 2816–2831, 1998.

[14] W. Yu and J. M. Cioffi, "FDMA capacity of Gaussian multiple-access channels with ISI," *IEEE Trans. Commun.*, vol. 50, no. 1, pp. 102–111, 2002.

[15] Z. Wang and G. B. Giannakis, "Wireless multicarrier communications: where Fourier meets Shannon," *IEEE Signal Processing Mag.*, vol. 17, no. 3, pp. 29–48, 2000.

[16] W. C. Jakes Jr., *Microwave Mobile Communications*, John Wiley & Sons, New York, NY, USA, 1974.

[17] A. Leon-Garcia, *Probability and Random Processes for Electrical Engineering*, Addison-Wesley, Reading, Mass, USA, 1994.

[18] D. G. Luenberger, *Optimization by Vector Space Methods*, John Wiley & Sons, New York, NY, USA, 1969.

[19] S. Verdú, *Multiuser Detection*, Cambridge University Press, Cambridge, UK, 1998.

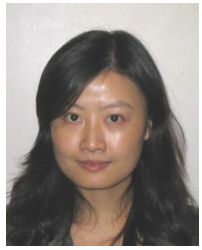

Mizhou Tan received the B.S. and M.S. degrees, both in electrical engineering, from Sichuan University, Chengdu, China, in 1993 and 1996, respectively, and a Ph.D. degree in electrical engineering from New Jersey Institute of Technology, Newark, NJ, in 2004. Currently, she is a Wireless Systems Engineer in Agere Systems, Allentown, Pa. Her research interests include multicarrier modulation systems, optimal power control for successive interference cancellation, peak-to-average power ratio reduction, and adaptive transmission.

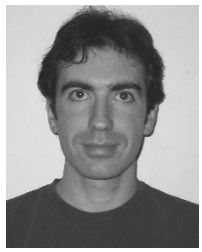

Christian Ibars received degrees in electrical engineering from Universitat Politecnica de Catalunya, Barcelona, Spain, and Politecnico di Torino, Torino, Italy, in 1999, and a Ph.D. degree in electrical engineering from the New Jersey Institute of Technology, Newark, NJ, in 2003. Since then he has been with the Centre Tecnològic de Telecomunicacions de Catalunya, Barcelona, Spain. His current research interests include wireless multiuser communications, CDMA, OFDM, and interference cancellation.

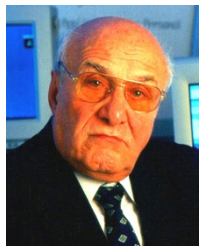

Yeheskel Bar-Ness received the B.S. and M.S. degrees in electrical engineering from the Technion, Israel, and the Ph.D. degree in applied mathematics from Brown University, Providence, RI. He is a Distinguished Professor of electrical and computer engineering and Foundation Chair of Communications and Signal Processing Research Center at the New Jersey Institute of Technology (NJIT), Newark. He is also the Executive Director of the Center for Communications and Signal Processing Research (CCSPR). After working in the private sector, he joined the School of Engineering, Tel Aviv University, in 1973. Between September 1978 and September 1979, he was a Visiting Professor at Brown University. He came to NJIT from AT&T Bell Laboratories in 1985. Current research interests include design of OFDM and MC-CDMA, adaptive processing for UWB, adaptive array and spatial interference cancellation, and signal separation for multiuser personal, indoor, and mobile wireless communications. He published numerous papers in these areas. He serves on the Editorial Board of WIRED Magazine, was the founding Editor-in-Chief of IEEE Communication Letters, and was an Associate and Area Editor for IEEE Transactions on Communications. He has been the Technical Chair of several major conferences and symposiums and was the recipient of the Kaplan Prize (1973), which is awarded annually by the Government of Israel to the ten best technical contributors.